



HEAT TRANSFER IN THREE-DIMENSIONAL RECTANGULAR CAVITIES WITH PINS

Zerrin SERT¹, Çisil TİMURALP² and Mesut TEKKALMAZ³

Eskisehir Osmangazi University, Mechanical Engineering Department, Eskisehir, Turkey

¹zbocu@ogu.edu.tr, ²cisil@ogu.edu.tr, ³tmesut@ogu.edu.tr

(Geliş Tarihi: 14.08.2017, Kabul Tarihi:08.02.2017)

Abstract: The interaction of natural convection with thermal radiation in three dimensional rectangular cavities with gray surfaces is studied numerically. The cavity is heated and cooled from the vertical opposing isothermal walls while all other side walls are adiabatic. The pins are placed to the active wall. The fluid is nonparticipating air ($Pr=0.71$), and the flow of air is assumed to be laminar. The fluid properties are taken to be constant at mean values, except for the density for which the Boussinesq approximation is employed. The governing flow, energy and the radiative transfer equations are solved by a commercial CFD code-ANSYS. The convection terms are discretized using a second order upwind scheme, and SIMPLE algorithm is adapted as the solution algorithm. The surface to surface (S2S) model is used for radiative heat transfer simulations. The Rayleigh number (Ra), the surface emissivity (ϵ), the number of pins, the dimensionless pin length and diameter ($B=b/H$ and $D=d/H$), the slenderness of the cavity (W/H) are variable parameters of this study. The slenderness ratio of $W/H=0.5, 1.0$ and 2.0 are considered. Enclosure with pin arrangements of 9, 13, 17, 21 and 25 are considered. The Rayleigh number, the surface emissivity, the dimensionless pin lengths and diameters are varied in the following intervals $10^3 \leq Ra \leq 10^6$, $0.0 \leq \epsilon \leq 1.0$, $0.05 \leq B \leq 0.6$, $0.025 \leq D \leq 0.1$, respectively. The mean Nusselt numbers for convection and radiation, as well as total, were computed as a function of the Rayleigh number for each case. Also the flow and temperature distribution for some cases have been presented and discussed.

Keywords: Three-dimensional, Natural convection, S2S Radiation, Rectangular cavities.

PİMLİ ÜÇ BOYUTLU DİKDÖRTGEN KUTULARDA ISI TRANSFERİ

Özet: Üç boyutlu gri yüzeyli dikdörtgen geometriye sahip kutularda termal radyasyon ile doğal taşınımın etkileşimi sayısal olarak incelenmiştir. Dikdörtgen kutuda dikey karşıt izotermal duvarlar ısıtılıp soğutulurken, diğer tüm duvarlar yalıtılmıştır. Pimler sıcak duvara eklenmiştir. Katılımcı olmayan ortamda akışkanın hava ($Pr=0.71$) ve akışın laminar olduğu kabul edilmiştir. Boussinesq yaklaşımının kullanıldığı yoğunluk dışındaki tüm termodinamik özelliklerinin sabit olduğu varsayılmıştır. Momentum, enerji denklemleri ve radyasyon transferi ticari CFD kodu ANSYS ile çözülmüştür. Taşınım terimlerinin ayrıştırılmasında ikinci dereceden ayrıştırma şeması, çözüm yöntemi olarak da SIMPLE algoritması ve yüzey ışınım hesabında S2S (Surface to Surface) ışınım modeli kullanılmıştır. Rayleigh sayısı (Ra), yüzey emissivitesi (ϵ), pim sayısı, boyutsuz pim çapları ($D=d/H$) ve uzunlukları ($B=b/H$), dikdörtgen kutunun genişlik yükseklik oranı (W/H) parametrik olarak değiştirilmiştir. Üç boyutlu kutunun, incelik oranı, $W/H=0.5, 1.0$ ve 2.0 olarak ele alınmıştır. Kutudaki pimlerin sayısı ise 9, 13, 17, 21 ve 25 olarak değiştirilmiştir. Rayleigh sayısı, yüzey emissivitesi, boyutsuz pim uzunlukları ve çapları, sırasıyla $10^3 \leq Ra \leq 10^6$, $0.0 \leq \epsilon \leq 1.0$, $0.05 \leq B \leq 0.6$, $0.025 \leq D \leq 0.1$, değer aralıklarında değiştirilmiştir. Ortalama taşınım, radyasyon ve toplam Nusselt sayıları, her durum için Rayleigh sayısının bir fonksiyonu olarak hesaplanmıştır. Ayrıca ele alınan tüm durumlar için akış ve sıcaklık dağılımları verilmiş ve tartışılmıştır.

Anahtar kelimeler: Üç boyutlu, Doğal taşınım, S2S Işınım, Dikdörtgen kutular.

NOMENCLATURE

B	dimensionless pin length	N_r	Conduction-radiation number [$= \sigma T_h^4 H / k \Delta T$]
b	length of pin, [m]	Nu	mean Nusselt number defined by Eq. (4)
D	dimensionless pin diameter	P	Pressure, [Pa]
d	diameter of pin, [m]	Pr	Prandtl number, [$= \nu / \alpha$]
g	Earth's gravitational acceleration, [m/s^2]	q	Heat flux [W/m^2]
H	height of enclosure, [m]	Q	Dimensionless heat flux
k	unit vector in z-direction	Ra	Rayleigh number [$= g \beta (T_h - T_c) H^3 / \nu \alpha$]
n	perpendicular direction	T	Temperature, [K]
		V	Dimensionless Velocity

W width of enclosure, [m]

Greek Symbols

ε Surface emissivity

α Thermal diffusivity, [m²/s]

β Thermal expansion coefficient, [1/K]

θ Dimensionless temperature $[(T-T_c)/(T_h-T_c)]$

ν Kinematic viscosity, [m²/s]

ρ Density, [kg/m³]

σ Stefan-Boltzmann constant [5.67x10⁻⁸ W/m²K⁴]

Subscripts

c cold

c convection

h hot

r radiation

t total

INTRODUCTION

Natural convection is one of the processes relating mass and thermal transport processes involved in many applications, such as solar collectors, power plants, cooling of electronic equipments, nuclear reactors, aerospace systems, fire hazards, and building engineering etc. For this reason, natural convection inside cavities has been and is still being investigated both experimentally and theoretically for the last several decades. The majority of the published studies have neglected the radiation transfer phenomena. However, the effects of radiation transfer become important due to the nature of the coupling between temperature and flow fields as well as enclosure configuration.

Numerical analysis of natural convection in 3D cavities (with fins or pins attached to its walls) has become more common with the continuous development of computer technology in the last decade. Da Silva and Gosselin (2005) studied heat transfer by natural convection in a 3D cavity with a pin on the hot wall. They reported that the pin aspect ratio had almost no effect on the heat transfer, and the heat transferred to the fluid increased steadily with the pin length. Frederick and Moraga (2007) numerically simulated 3D natural convection in a cubical enclosure with a pin on the active wall. As a result, $10^5 \leq Ra \leq 10^6$, it was found out that the specific pin width was more important than full pin length. Bocu and Altac (2011) numerically investigated the heat transfer of laminar natural convection in 3D rectangular cavities with pins attached to the hot wall. In this work, it was shown that the pin length had an important effect on heat transfer.

In literature, most studies deal with either pure radiation or pure natural convection heat transfer. On the other hand, the majority of the numerical studies, which deal with combined radiation and convection, are done for 2D enclosures. Balaji and Venkateshan (1993) studied numerically the combined surface radiation and natural convection in a square enclosure. Their work emphasized the importance of surface radiation at low emissivity and temperature level. Balaji and Venkateshan (1994) also studied numerically combined

natural convection and surface radiation in a filled air square cavity. Correlations are suggested for both radiation and convection heat transfer rates. Sen and Sarkar (1995) numerically studied the combined laminar natural convection and surface radiation in a differentially heated square enclosure. They found that the isotherms spread considerably apart near the active wall when radiation was present and as variable property convection was concerned, the symmetry of the mid-plane vertical velocity and temperature fields were lost. Akiyama and Chong (1997) numerically analyzed the natural convection and surface radiation heat transfer from gray surfaces in a square enclosure with air as the working fluid. They showed that the mean radiative Nusselt number increased dramatically when the emissivity was raised, and the radiation heat transfer was effective in overall heat flux at larger emissivity. Mezrhab and Bchir (1998) obtained the problem of combined heat transfer to the 2D enclosure with adding a thick partition located vertically close to the hot wall. They found out that radiation had a significant effect of the heat transfer and flow in the enclosure. Ben-Nakhi and Chamkha (2006) investigated the effect of length and the thin pin inclination on the natural convection in a square enclosure. The results showed that the Rayleigh number, the inclination angle and the length of thin fin had significant influences on the mean Nusselt number of the heated wall. Combined free convection and surface radiation in a square cavity with a non-uniformly heated plate is studied numerically by Saravanan and Sivaraj (2015). They discussed the influence of non-uniform and uniform heating of the plate on the total and convective heat transfer rates.

Vivek et al. (2012) numerically studied the effects between natural convection and thermal radiation heat transfer in tilted air filled square-shallow enclosures for a wide range of tilt angles. The interaction effects between radiation and convective heat transfer are stronger in shallow enclosures than square enclosures. Bouali et al. (2006) numerically examined the heat and fluid flow in the presence of surface radiation and natural convection in inclined rectangular enclosures with a centered inner body. They found that the increasing the inclination angle reduced the total heat transfer in the enclosure, and the surface radiation increased the total Nusselt number. Rabhi et al. (2008) have numerically studied the radiation and natural convection interactions in a differentially heated inclined enclosures with single and multiple partition plates. As a result, the total heat transfer in the enclosure is increased with radiative heat flux and reduced with increasing the number of partitions. Turbulent natural convection coupled with surface radiation has been studied numerically in air filled rectangular enclosures heated from bottom and cooled from other walls by Sharma et al. (2007). A correlation for the mean convection Nusselt number was derived in terms of Rayleigh number and aspect ratio.

In recent years, experimental studies on natural convection and thermal radiation heat transfer have been carried out in enclosures with pins. Sparrow and Vemuri (1985) experimentally investigated combined radiation and natural convection heat transfer in an enclosure with many of pins. It was found that the influence of radiation was important for longer fins for small enclosure temperature differences. Alessio and Kuminski (1989) studied radiation and natural convection heat transfer from an array of inclined pins experimentally. The effects of the horizontal angle of the pin, the pin length and intensity were investigated. The results indicated that radiation heat transfer was more significant at low Grashof numbers, large inclination angles and longer pin lengths. Zografos and Sunderland (1990) examined natural convective heat transfer from uniform and non-uniform pin arrays experimentally. The pin diameter spacing ratio convective heat transfer affecting is the most important parameter. In additionally, the inclination angle less than 30° from the vertical on arrangement was relatively small on the convective performance. Rao Rammohan and Venkateshan (1996) performed an experimental study of natural convection and surface radiation in horizontal pin arrays. The effects of base temperature, the pin surfaces emissivity, spacing and height were presented and correlations are suggested. Ramesh and Venkateshan (1999) experimentally studied the interaction of natural convection and thermal radiation with heat transfer in square enclosure having differentially heated side walls and adiabatic horizontal walls. Correlations for convection, radiation and total Nusselt numbers were reported. Sertkaya et al. (2011) studied experimentally the effects of orientation angle in finned surfaces in combined free convection and thermal radiation heat transfer. They observed that the heat transfer rates and the effect of pin were decreased with increasing orientation angle.

Attaching fin/pin arrays to the hot walls is commonly used in electronic cooling processes. Colomer et al. (2004) numerically investigated 3D natural convection and radiation heat transfer for participating and transparent media in a differentially heated enclosure using the discrete ordinates method. For nonparticipating media, the connection between the Navier-Stokes equations and radiation was done over the radiation between surfaces. The effects of Rayleigh and Planck numbers and optical thickness on heat transfer rates presented in this study. They concluded that the radiation significantly increased the heat flux in a transparent medium and for a specific Planck number and fixed reference temperature ratio, the contribution of radiation stayed almost stable for a set of Rayleigh numbers. Combined natural convection and radiation in a cavity was also studied numerically by Kuznetsov and Sheremet (2009). They analyzed the effect of Grashof number, the optical thickness, the heat conductivity ratio and the transient factor. Martyushev and Sheremet (2014) numerically presented natural convection combined with thermal surface radiation in a cubical enclosure with finite thick solid walls at constant

temperature heat source. Correlations were found for mean convection and radiation Nusselt numbers for Rayleigh number, the surface emissivity and the thermal conductivity ratio. Dogan et al. (2014) numerically studied the natural convective and radiative heat transfer from various shaped thin pin-arrays on a horizontal plate. They showed that the optimum-shaped pin array had more mean heat transfer coefficient than the rectangular pin array. Sahray et al. (2010) experimentally and numerically studied the influence of pin height and pin population density of horizontal-base pin sinks in natural convection and radiation. By separating the convection from the radiation, a correlation is obtained, involved the Nusselt and Rayleigh numbers. Das et al. (2018) investigated experimentally augmentation of convection heat transfer through a heated fin arrangement in a rectangular enclosure. The variable parameters in their work are as follows: fin height ($12.5\text{mm} \leq L \leq 37.5\text{mm}$), fin spacing ($25\text{mm} \leq S \leq 100\text{mm}$) and Rayleigh number ($360000 \leq Ra \leq 680000$).

For increasing heat transfer from high performance logic chips, generally heat sinks are placed on surfaces to increase surface area. It is also important to keep the chip operating temperature at a certain value. For this reason, it is necessary to use effective cooling in electronic equipment. The effect of radiative heat transfer is between 25 to 40% of total heat transfer from fin arrays in finned heat sink (Sparrow and Vemuri, 1985). Therefore, in order to maximize heat transfer, the effects of pin parameters (such as pin length and diameter, number of pins, etc.) need be investigated. The above mentioned efforts, however, were mainly been studied to investigating the natural convection in enclosures, and partly involved the effect of pin parameter to natural convection and surface radiation in enclosures. The objective of this study is to computationally analyze the heat transfer rates due to natural convection coupled with radiation in a 3D cavities, $W/H=2.0$, $W/H=1.0$ and $W/H=0.5$, with pin array on the hot wall. The cavity is heated from the lateral wall (where the pin array is attached) while it is cooled from the opposite wall. The study is carried out for the range of the Rayleigh numbers from 10^3 to 10^6 with air as a working fluid ($Pr=0.71$). The number of pins of 9, 13, 17, 21 and 25 in various arrangements are considered in this study. The diameter and the length of the pins are also varied respectively in $0.025 \leq D \leq 0.1$ and $0.05 \leq B \leq 0.6$ intervals. The emissivity of the cavity walls, including pins, is also varied between 0.0 and 1.0. This study explores the effects of radiation with respect to no-radiation cases. The Nusselt numbers due to convection and radiation are computed over the cold surface and compared for the variable parameters.

PHYSICAL AND MATHEMATICAL MODEL

A schematic illustration of the physical problem investigated is given in Figure 1, where x , y and z are the Cartesian coordinates, and H and W are the lengths of the cavity. The fluid is air ($Pr=0.71$). The left vertical

wall (surface, $x=0$), including the pins, are maintained at an elevated constant temperature T_h , while the opposite vertical wall $x=W$ is kept at constant cooler temperature T_c . All the other walls are adiabatic. The surface emissivity of the walls is assumed to be the same. The thermophysical properties of air are assumed constant except for the density for which Boussinesq approximation is used.

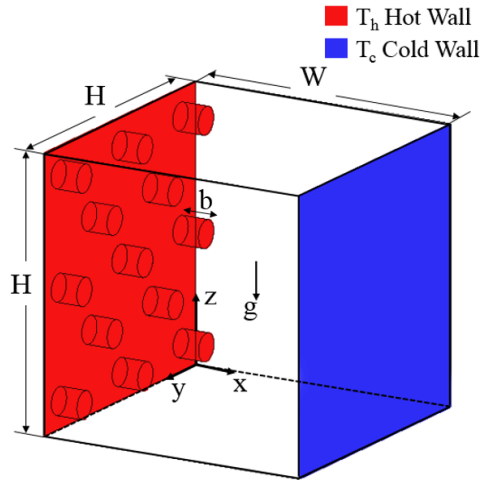


Figure 1. Physical model and the coordinate system.

The governing flow and energy equations are given as, for the continuity equation

$$\nabla \cdot \mathbf{V} = 0 \quad (1)$$

for the momentum equations

$$(\mathbf{V} \cdot \nabla) \mathbf{V} = -\frac{1}{\rho} \nabla P + \nu \nabla^2 \mathbf{V} - g\beta(T - T_0) \mathbf{k} \quad (2)$$

for the energy equation

$$(\mathbf{V} \cdot \nabla) T = \alpha \nabla^2 T \quad (3)$$

where \mathbf{V} is the velocity, ρ is the density, P is the pressure, ν is the kinematic viscosity, β is the thermal expansion coefficient, T is the temperature, α is the thermal diffusivity, \mathbf{k} is the unit vector in z -direction. Rayleigh and Prandtl numbers are described as $Ra = g\beta(T_h - T_c)H^3/\nu\alpha$ and $Pr = \nu/\alpha$, respectively.

The hot and cold surfaces are isothermal, and all the other walls assumed to be adiabatic. All walls are impermeable no-slip boundaries. The boundary conditions can be stated as:

$$\text{For hot wall, } T = T_h, \quad \mathbf{V} = 0$$

$$\text{For cold wall, } T = T_c, \quad \mathbf{V} = 0 \quad (4)$$

$$\text{For adiabatic walls, } \partial\theta/\partial\mathbf{n} - N_r Q_r = 0, \quad \mathbf{V} = 0$$

where \mathbf{n} is the normal direction. N_r is conduction-radiation number which is defined as $N_r = \sigma T_h^4 H/k\Delta T$. $Q_r = q_r/\sigma T_h^4$; Q_r is the dimensionless radiation heat flux on the corresponding insulated wall and q_r is also the radiation heat flux on the corresponding insulated

wall. In the discussions, the dimensionless temperature will be used which will be defined as $\theta = (T - T_c)/(T_h - T_c)$.

Figure 2 depicts typical cylindrical pin arrangements. The number of pins of 9, 13, 17, 21 and 25 are used in various arrangements. The pins of diameter d and length b are placed on the hot wall (see Figure 1). The dimensionless pin diameter and length are expressed as $D=d/H$ and $B=b/H$. In the numerical simulations the dimensionless pin length and diameter are varied between $B=0.05-0.6$ and $D=0.025-0.1$.

The mean total Nusselt number for cold wall is calculated by,

$$Nu_t = Nu_c + Nu_r = \frac{q_c + q_r}{k(T_h - T_c)/H} \quad (5)$$

where q_c and q_r convection and radiation heat flux.

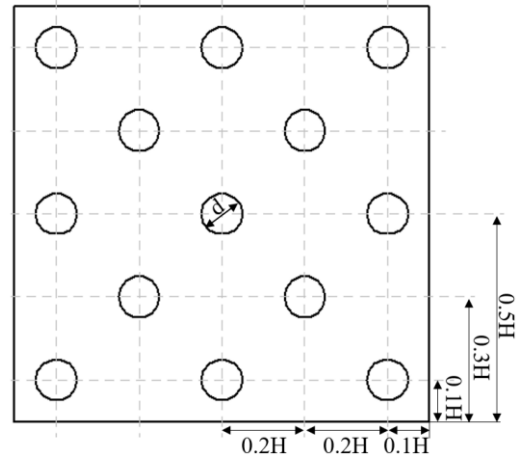


Figure 2. 13-pin-array arrangement.

NUMERICAL SOLUTION

Heat and fluid flow were simulated using standard $k-\epsilon$ and realizable $k-\epsilon$ models. It was observed that both heat and fluid flow were identical in the Ra number interval studied. Thus the flow was of air was assumed to be laminar natural convection regime. The continuity, momentum, energy and the radiation transfer equations are analyzed using Fluent®. The convection terms were discretized using “Second Order Upwind”, and SIMPLE algorithm was employed to solve coupled-transport equations. In assessing the radiative transfer between the walls, the surface to surface (S2S) heat transfer model was employed. The convergence criterion was set to 5×10^{-5} for all equations. Three cases of rectangular cavities are considered in this study: $W/H=0.5$, $W/H=1.0$ and $W/H=2.0$.

In order to obtain meaningful numerical solutions, meshing the computational domain is a crucial first step. To decide on the optimum grid configuration, a comparison of the mean (convective) Nusselt numbers with the reported results for a bare cubic cavity for various Rayleigh numbers is provided in Table 1. Also In Table 2, both radiative, convective and mean total

Nusselt numbers obtained for three grid configurations are tabulated for $\varepsilon=1.0$.

Three different grids were adapted depending on the Rayleigh number. Initially the cavities were meshed equally-spaced homogeneous grids (hexahedral elements). This grid configuration is generally sufficient for low Rayleigh number cases. However, as the Rayleigh number increases, thermal and hydrodynamic boundary layers along the hot and cold walls become thinner. To be able to capture both of these boundary layers is crucial to accurately compute the heat transfer rates. For this reason, the grids were condensed near the

cold and hot walls through "adaption" procedure—a feature available in Fluent®. The mean Nusselt numbers have satisfactorily converged to the values predicted in the literature. When the computed and the reference Nusselt values (Colomer et al., 2004) are compared, the relative errors in the mean Nusselt values were within 3% level. For $80 \times 80 \times 80$ homogeneous grid size, the relative error was 0.5% in comparison to $50 \times 50 \times 50$ grid size with adaption. Consequently, the optimum grid configuration was determined $50 \times 50 \times 50$ grid size with adaption.

Table 1. Verification of the mean Nusselt numbers for bare cube without radiation.

Ra	Nu						
	Frederick and Moraga (2007)	Colomer et al. (2004)	Bocu and Altac (2011)	Tric et al. (2000)	Present Study		
					50×50×50 with adaption (596581 nodes)	80×80×80 (531441 nodes)	100×100×100 (1030301 nodes)
10 ³	1.07124	1.055	1.0706	1.0700	1.050	1.045	1.050
10 ⁴	2.05703	2.030	2.0575	2.0542	2.021	2.014	2.014
10 ⁵	4.35340	4.334	4.3598	4.3370	4.275	4.271	4.271
10 ⁶	8.74003	8.862	8.7945	8.6407	8.587	8.600	8.600

Table 2. Grid sensitivity table for bare cube with radiation ($\varepsilon = 1.0$).

Ra	Nu											
	Colomer et al. (2004)			Present Study								
				50×50×50 with adaption (596581 nodes)			80×80×80 (531441 nodes)			100×100×100 (1030301 nodes)		
	Nu _t	Nu _r	Nu _c	Nu _t	Nu _r	Nu _c	Nu _t	Nu _r	Nu _c	Nu _t	Nu _r	Nu _c
10 ³	4.596	3.162	1.434	4.838	3.422	1.416	4.813	3.416	1.397	4.838	3.422	1.417
10 ⁴	5.295	3.233	2.062	5.506	3.484	2.022	5.480	3.478	2.002	5.506	3.484	2.023
10 ⁵	7.368	3.385	3.983	7.468	3.614	3.854	7.446	3.608	3.838	7.472	3.614	3.858
10 ⁶	11.67	3.568	8.102	11.498	3.772	7.726	11.49	3.765	7.730	11.49	3.772	7.726

RESULTS AND DISCUSSIONS

In Figure 3, for the surface emissivity $\varepsilon=0.0$ and 1.0 and the pins dimensions of a) $D=0.025$ and b) $D=0.1$, and $B = 0.1$, the variation of the mean total Nusselt number with the Rayleigh number, pin numbers as well as pin arrangements are depicted. It is clear that the heat transfer will increase as the pins surface area increases. However, it is observed that the increasing surface area by increasing the number of pins has little effect on heat transfer. As the air is heated in the vicinity of the pins, air ascends vertically, the cold air fills the vacated region. Thus, the temperature difference between air and the bottom pin-row is higher, while the temperature difference between the top pin-rows and the air becomes lower. Therefore, the heat transfer from the bottom pin-row is greater than the heat transfer from the top pin-row. This results in thickening of thermal boundary layer from the bottom to the top. As a result as the number of pins is increased, the temperature gradient between the isothermal pins and the surrounding air

decreases. In the case of $D=0.025$, $Ra=10^5$ and $\varepsilon=1.0$ (Figure 3a), the maximum relative percentage change of Nu_t values for 9-pin and 25-pin arrangement is 1.26%. Similarly, in the case of $D=0.1$, $Ra=10^5$ and $\varepsilon=1.0$ (Figure 3b), the maximum relative percentage change in Nu_t for 9-pin and 25-pin arrangement is about 3.5%. Noting that the number of pins and their configuration do not significantly effects the heat transfer rates, it has been decided to carry out the flow and heat transfer analysis with the 13 pin-configuration presented in Figure 2.

In Figure 4, for $\varepsilon=0.0, 0.5$ and 1.0 , the temperature distribution of $Ra=10^5$, $W/H=1.0$, $D= 0.05$ and $B=0.1$ case is illustrated along $x/H=0.05$ and $y/H=0.1$ planes. For walls with low surface emissivity, a large area due to the pins is observed to warm up the air. With increasing the surface emissivity the warm region shrinks and confined to the upper part of the cavity, and the temperature gradients around the pins increase which lead to increased convection heat transfer rate.

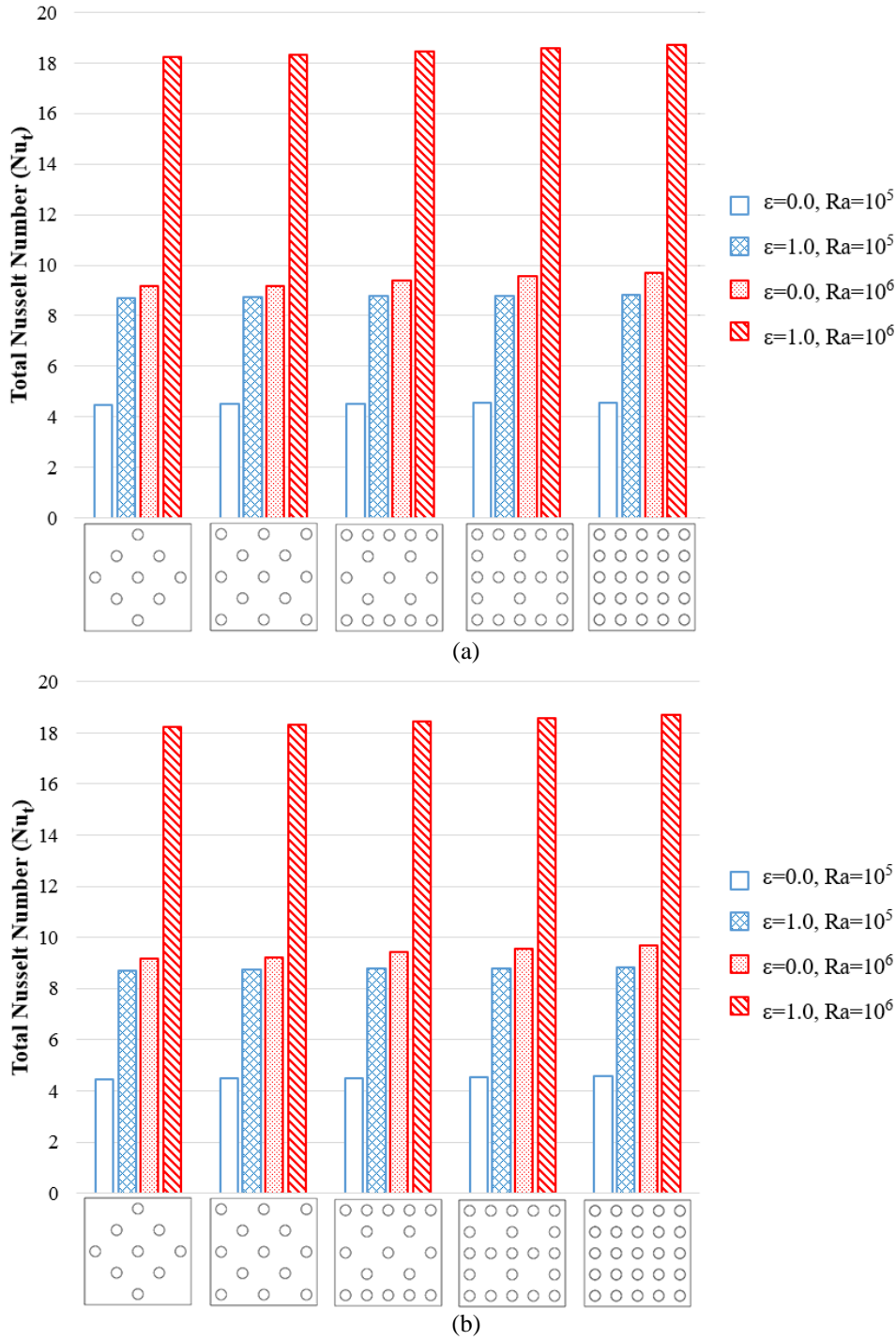


Figure 3. Variation of the total mean Nusselt number with the numbers of pin and the Rayleigh number for $B = 0.1$ and a) 0.025 and b) $D=0.1$.

In Figure 5, for $\varepsilon = 0.5$, $W=1.0$, $D=0.025$ and $B=0.1$, isotherms and path lines (coloured by temperature) are shown for all Rayleigh numbers considered. As air receives heat, its density decreases, and in turn the hot air rises to the top of the cavity. For $Ra=10^3$, the isotherms are almost vertical which indicates a weak circulation. As the Rayleigh number increases, the circulation gains strength, and the isotherms deviate further from nearly parallel formation (Fig5. b and c). At $Ra=10^5$, the isotherms tend to be horizontal in the middle region of the cavity. However, with increasing

Rayleigh number, the strength of the circulation increases, and the thermal boundary layers are formed alongside the hot and cold walls. As the isotherms coalesce near the walls, the temperature gradient at these walls increase which in turn increases the heat transfer rate. When the path lines are examined, with the increasing Rayleigh number, irregularities in the flow increase due to three-dimensionality of the cavity and the flow, thus providing a mixing in the cavity which also leads to increase in the heat transfer.

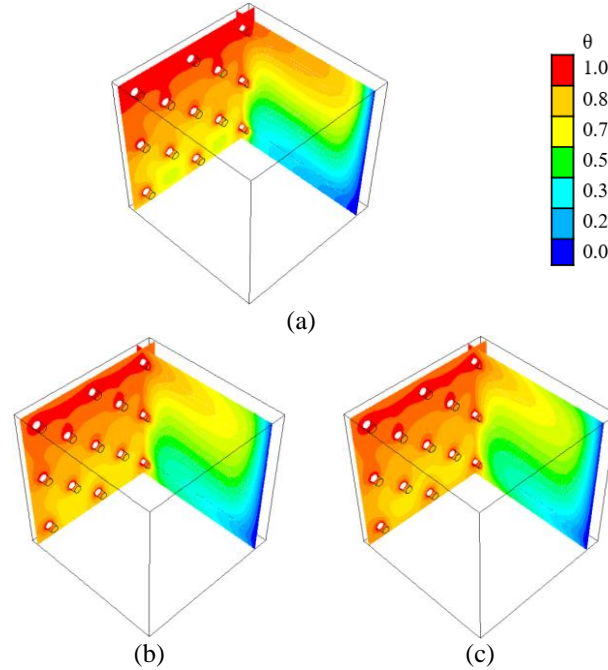


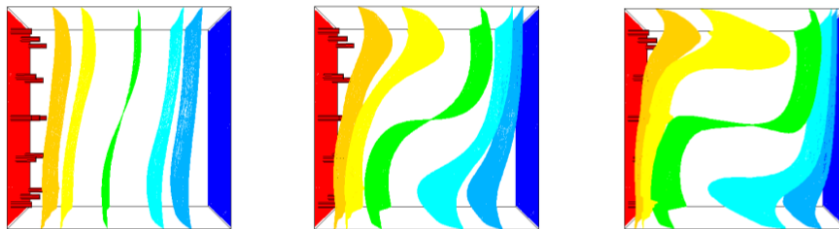
Figure 4. Temperature distribution for for a) $\varepsilon = 0.0$, b) $\varepsilon = 0.5$, c) $\varepsilon = 1.0$ of $Ra=10^5, W/H=1.0, D= 0.05$ and $B=0.1$ case. (Along $x/H=0.05$ and $y/H=0.1$ planes).

In Figure 6, for $\varepsilon = 1.0$, $Ra=10^5$, $D=0.05$ and $B=0.1$, isotherms are shown for three slenderness ratios: $W/H=0.5, 1.0$ and 2.0 . The height of the cavities is kept constant while widths are varied accordingly. The difference in these three situations arises from increasing the distance between the hot and cold walls. As W/H is increased, the heat transfer rates (mean convective Nusselt numbers) decrease since the interaction between the hot and cold walls is hindered due to the volume and the distance of the cavity. The rectangular cavity case of $W/H=2.0$ allows less heat transfer in comparison to $W/H=1.0$ and the other rectangular cavity case of $W/H=0.5$.

The Figure 7, for $B=0.1$ and $\varepsilon=0.5$, the variation of mean total and radiative Nusselt numbers as a function of Ra number, W/H and D is depicted. At low Rayleigh numbers, heat transfer is dominated by conduction. However, convection plays an important role in comparison to conduction as Rayleigh number increases gradually. The mean total and radiative Nu numbers

steadily increase with increasing Rayleigh number for each case. Furthermore, as the number of Rayleigh increases, the change in heat transfer rate becomes more step. For $B=0.1$ and $\varepsilon=0.5$, the heat transfer rate increased from 1.85% to 7.1% compared to $D=0.1$ and $D=0.025$ in all slenderness ratio of 3D cavity.

In Figure 8, for $D=0.025$, $W/H=1.0$ and $\varepsilon=0.5$, the variation of mean total Nusselt number with the dimensionless pin lengths and the Rayleigh number are depicted. As the dimensionless pin length increases, the mean total Nusselt number depict nearly a linear increase. This increase is more pronounced with increasing Rayleigh number. This increase is associated with increased hot surface area due to addition of the pins. In comparison to the bare cavity for $Ra=10^6$, the relative increase in the mean total Nusselt number is about 1.02%, 4.65%, 8.25%, 12.75%, 21.87% and 35.75% for $B=0.05, B=0.1, B=0.15, B=0.2, B=0.3$ and $B=0.6$, respectively.



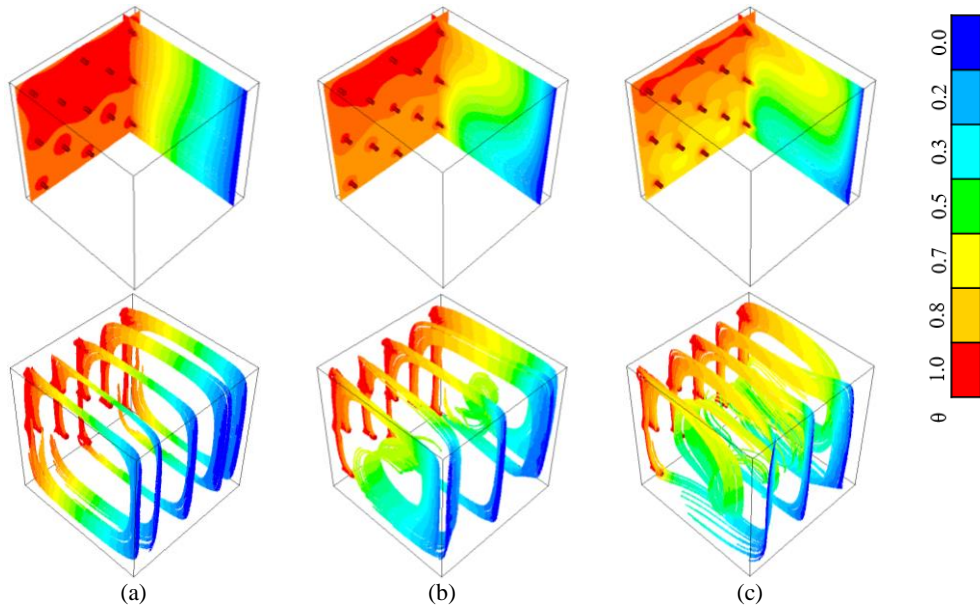


Figure 5. The effect of Rayleigh number on isothermal surfaces (top), temperature distribution along $x/H=0.05$ and $y/H=0.1$ planes (middle) and path lines (coloured by temperature) (below) for, $W=1.0$, $D=0.025$, $B=0.1$ and a) $Ra=10^3$, b) $Ra=10^4$, c) $Ra=10^5$.

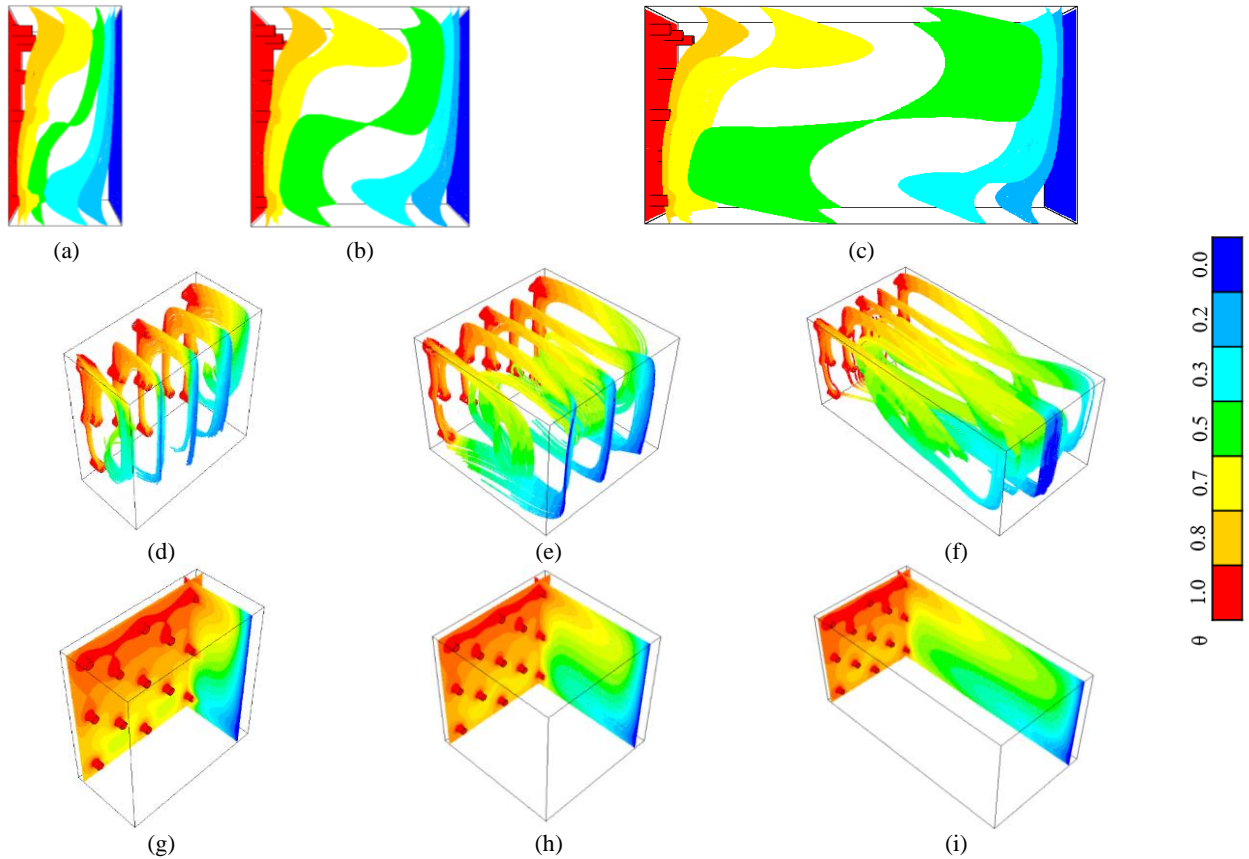


Figure 6. Isothermal surfaces (top), path lines (coloured by temperature) (middle) and temperature distribution along $x/H=0.05$ and $y/H=0.1$ planes (below) for $\varepsilon = 1.0$, $Ra=10^5$, $D=0.05$, $B=0.1$ and three slenderness ratios of the 3D cavity a,d,g) $W/H=0.5$, b,e,h) $W/H=1$, c,f,i) $W/H=2.0$.

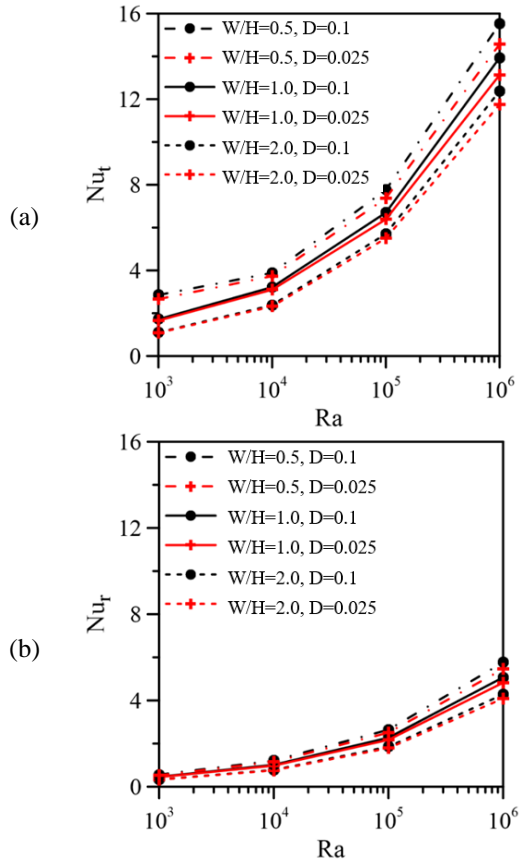


Figure 7. The mean Nusselt numbers variation with Ra number, the dimensionless pin diameters and the slenderness ratio of the 3D cavity for $B=0.1$ and $\varepsilon=0.5$, a) for total, b) for radiation.

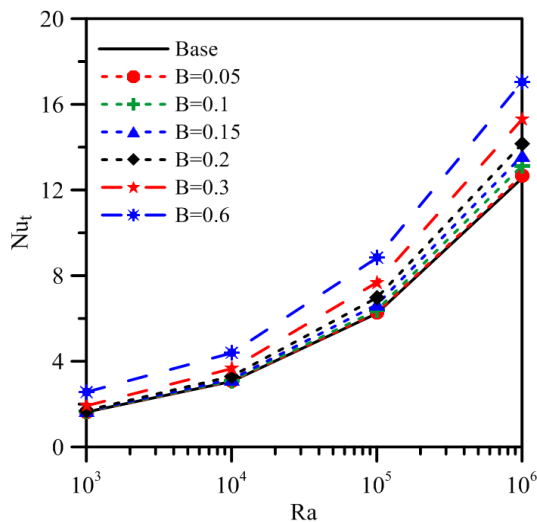


Figure 8. Variation of mean total Nusselt number with the dimensionless pin lengths and the Rayleigh number for $D=0.025$, $W/H=1.0$ and $\varepsilon=0.5$.

In the Figure 9, for $B=0.1$ and $D=0.05$, the variation of mean total, radiative and convective Nusselt numbers are depicted as a function of ε , Ra number and W/D . When Rayleigh number is 10^4 and 10^5 , as the surface emissivity is increased, Nu_r and Nu_t increase by a small

amount with W/H slenderness ratio. However, for $Ra=10^6$, Nu_r and Nu_t depict steady increase with increasing surface emissivity while Nu_c is more less constant for $W/H < 1.0$ it decreases slightly with increasing W/H . When the Rayleigh number is 10^4 and 10^5 , the mean convective Nusselt number remains constant with the emissivity while it decreases with increasing W/H . In high Rayleigh number and high surface emissivity, radiation effect is more apparent. In all cases, as W/H slenderness ratio decreases, the mean total Nusselt number increases mainly due to radiation heat transfer.

CONCLUDING REMARKS

A computational analysis of laminar natural convection and thermal surface radiation in 3D rectangular cavities with pin arrays attached to the hot wall has been carried out. The flow and heat transfer parameters inside the cavity have been investigated for a range of the surface emissivity ($0.0 \leq \varepsilon \leq 1.0$) and Rayleigh number ($10^3 \leq Ra \leq 10^6$). The slenderness of the 3D cavity ($W/H=0.5, 1.0, 2.0$) and the dimensionless pin lengths and diameters ($B=0.05-0.6$ and $D=0.025-0.1$) were varied, and mean convective and radiative Nusselt numbers over the cold surface were calculated for all statement. The results of this study can be summarized as follows:

- 1) When numerous pins are attached to an active wall, the number of pins and their configurations has very little effect on heat transfer.
- 2) With increasing Rayleigh number, the circulation within the 3D cavity gains strength, causing velocity and temperature gradients, hereby increasing heat transfer rates.
- 3) The mean total and radiative Nu number increase with increasing the pin length and diameter and the surface emissivity of the cavity/pin walls. However, the mean convective Nu number slightly decrease with increasing the surface emissivity.
- 4) With increasing the slenderness of the 3D cavities (W/H), heat transfer rates decrease for all case.
- 5) Radiation is the predominant mechanism of heat transfer and significantly alters the temperature distribution and flow patterns, raising temperatures in the inner region of the 3D rectangular cavity. We can remark that at $Ra=10^3$, the correlations of pure natural convection are used correctly. But the increase of the Rayleigh number and the surface emissivity leads to increase radiation effect. So at high Ra numbers, using the correlations of pure natural convection is lead into error. When the walls are black, there is an increase about twice as in the total Nusselt number according to pure natural convection case.

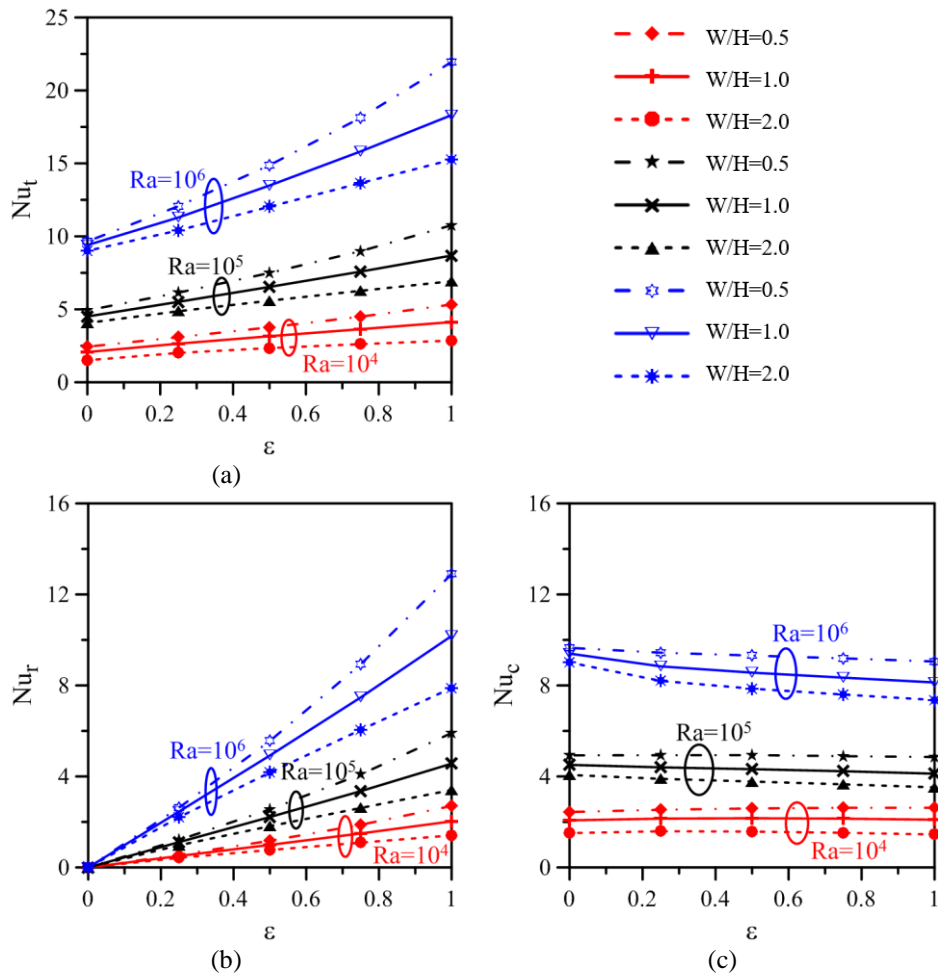


Figure 9. Variation of a)total, b)radiation and c)convection Nusselt number with the surface emissivity at $B=0.1$ and $D=0.05$.

REFERENCES

Akiyama M., and Chong Q.P., 1997, Numerical analysis of natural convection with surface radiation in a square enclosure, *Numer. Heat Tr. A-Appl*, 32, 419-433.

Alessio M.E., and Kuminski D.A., 1989, Natural convection and radiation heat transfer from an array of inclined pin fins, *J. Heat Transf.*, 111(1), 197-199.

Balaji C., and Venkateshan S.P., 1993, Interaction of surface radiation with free convection in a square cavity, *Int. J. Heat Fluid Fl.*, 14(3), 260-267.

Balaji C., and Venkateshan S.P., 1994, Correlations for free convection and surface radiation in a square cavity, *Int. J. Heat Fluid Fl.*, 15(3), 249-251.

Ben-Nakhi A., and Chamkha A.J., 2006, Effect of length and inclination of a thin fin on natural convection in a square enclosure, *Numer. Heat Tr. A-Appl*, 50, 381-399.

Bocu Z., and Altaç Z., 2011, Laminar natural convection heat transfer and air flow in three-dimensional rectangular enclosures with pin arrays attached to hot wall, *Appl. Therm. Eng.*, 31, 3189-3195.

Bouali H., Mezrhab A., Amaoui H., and Bouzidi M., 2006, Radiation-natural convection heat transfer in an inclined rectangular enclosure, *Int. J. Therm. Sci.*, 45, 553-566.

Colomer G., Costa M., Consul R., and Oliva A., 2004, Three dimensional numerical simulation of convection and radiation in a differentially heated cavity using the discrete ordinates method, *Int. J. Heat Mass Tran.*, 47, 257-269.

Da Silva A.K., and Gosselin L., 2005, On the thermal performance of an internally finned three dimensional cubic enclosure in natural convection, *Int. J. Heat Mass Tran.*, 44, 540-546.

Das, D., Dwivedi, A., and Verma, S.P., 2018, Performance of heated pin fin arrangement in a rectangular cavity-An experimental approach, *J. Mech. Sci. Technol.*, 32(4), 1897-1903.

Dogan M., Sivrioglu M., and Yilmaz O., 2014, Numerical analysis of natural convection and radiation heat transfer from various shaped thin fin-arrays placed on a horizontal plate-a conjugate analysis, *Energ. Convers. Manage.*, 77, 78-88.

Frederick R.L., and Moraga S.G., 2007, Three-dimensional natural convection in finned cubical enclosures, *Int. J. Heat Fluid Fl.*, 28, 289-298.

Kuznetsov G.V., and Sheremet M.A., 2009, Conjugate natural convection with radiation in an enclosure, *Int. J. Heat Mass Tran.*, 52, 2215-2223.

Martyushev S.G., and Sheremet M.A., 2014, Conjugate natural convection combined with surface thermal radiation in a three-dimensional enclosure with a heat source, *Int. J. Heat Mass Tran.*, 73, 340-353.

Mezrhab A., and Bchir L., 1998, Radiation-natural convection interactions in partitioned cavities, *Int. J. Numer. Method H.*, 8, 781-799.

Rabhi M., Bouali H., and Mezrhab A., 2008, Radiation-natural convection heat transfer in inclined rectangular enclosures with multiple partitions, *Energ. Convers. Manage.*, 49, 1228-1236.

Ramesh N., and Venkateshan S.P., 1999, Effect of surface radiation on natural convection in a square enclosure, *J. Thermophys. Heat Tr.*, 13(3), 299-301.

Rammohan Rao V., and Venkateshan S.P., 1996, Experimental study of free convection and radiation in horizontal fin arrays, *Int. J. Heat Mass Tran.*, 39(4), 779-789.

Sahray D., Shmueli H., Ziskind G., and Letan R., 2010, Study and optimization of horizontal-base pin-fin heat sinks in natural convection and radiation, *J. Heat Transf.*, 132(1), 012503-012503-13.

Saravanan S., and Sivaraj C., 2015, Combined natural convection and thermal radiation in a square cavity with a nonuniformly heated plate, *Computer & Fluids*, 117, 125-138.

Sen S., and Sarkar A., 1995, Effects of variable property and surface radiation on laminar natural convection in a square enclosure, *Int. J. Numer. Method H.*, 5, 615-627.

Sertkaya A.A., Bilir S., and Kargıcı S., 2011, Experimental investigation of the effects of orientation angle on heat transfer performance of pin-finned surfaces in natural convection, *Energy*, 36, 1513-1517.

Sharma A.K., Velusamy K., Balaji C., and Venkateshan S.P., 2007, Conjugate turbulent natural convection with surface radiation in air filled rectangular enclosures, *Int. J. Heat Mass Tran.*, 50, 625-639.

Sparrow E.M., and Vemuri S.B., 1985, Natural convection/radiation heat transfer from highly populated pin fin arrays, *J. Heat Transf.*, 107(1), 190-197.

Tric E., Labrosse G., and Betrouni M., 2000, A first incursion into the 3D structure of natural convection of air in a differentially heated cubic cavity, from accurate numerical simulations, *Int. J. Heat Mass Tran.*, 43, 4043-4056.

Vivek V., Sharma A.K., and Balaji C., 2012, Interaction effects between laminar natural convection and surface radiation in tilted square and shallow enclosures, *Int. J. Therm. Sci.*, 60, 70-84.

Zografos A.I., and Sunderland J.E., 1990, Natural convection from pin fin arrays, *Exp. Therm. Fluid Sci.*, 3(4), 440-449.



Zerrin SERT She is an assistant Professor in the Department of Mechanical Engineering at Eskişehir Osmangazi University. She received her B.Sc., M. Sc. And Ph.D. from Eskişehir Osmangazi University. She deals with Computational Fluid Dynamics and Heat Transfer.



Çisil TİMURALP She received her B.Sc., M.Sc. and Ph.D. degrees in mechanical engineering from Eskişehir Osmangazi University. She is currently working as an Assist. Prof. in Mechanical Engineering Department in the same university.



Mesut TEKKALMAZ He was born in Eskişehir-Turkey in 1972. He graduated from Department of Mechanical Engineering of Eskişehir Anadolu University in 1994. He received the degree of MSc and PhD from Department of Mechanical Engineering of Eskişehir Osmangazi University in 1996 and 2003, respectively. He is associate professor of Mechanical Engineering Department in Eskişehir Osmangazi University.